# Dispersion Characteristics of EME Microstrip at First Higher Order

Ching-Kuo Wu, Yu-Chiao Chen, and Ching-Kuang C. Tzuang

Institute of Electrical Communication Engineering, National Chiao Tung University, Hsinchu, Taiwan,
e-mail: cktzuang@cc.nctu.edu.tw

*Abstract* — **The dispersion characteristics of the electric-magnetic-electric (EME) microstrip at the first higher order are presented. The EME microstrip consists of composite metals paralleling the electric and magnetic surfaces, where the magnetic surface is made of an array of coupled inductors. The dispersion curves obtained by matrix-pencil analyses are validated experimentally by the measured radiation patterns. The line width is reduced by 47.5%, compared to that of the conventional microstrip for the same onset frequency of the leaky mode. The EME microstrip is potentially useful for compact microstrip leaky-mode array design.**

## I. Introduction

In recent years, there has significant progress in the area of leaky-mode antennas derived from open mm-waveguides [1]-[4]. Additionally, printed microstrip antennas are simple in structure and easy to fabricate by lithography. They are low profile, light weight, low cost devices that are well suited as radiating elements for integrated antenna array systems [5]-[6].

Further reduction of circuit dimensions in passive devices, especially the antenna component, is important from the cost, performance and reliability point of view. Recently, applications of the photonic bandgap (PBG) structure or the periodic device have drawn much interest in physics and engineering [7]-[8]. A new PBG microstrip line called the EME (electric-magnetic-electric) microstrip was proposed, analyzed and tested by experiments [9]-[10]. The results show that the EME composite structure can be a low-loss, slow-wave line under the dominant mode operation. This paper, for the first time, investigates the dispersion characteristics of the first higher order mode of the EME microstrip which incorporates a PBG structure and experiences periodic perturbations on the strip line itself. The EME microstrip not only reduces the dimension by 47.5% but possesses all the inherent unique characteristics of uniform microstrip leaky-mode antennas, such as narrow fan beam and frequency scanning. Therefore, a compact and high performance integrated antenna array can be designed using the EME composite microstrip.

The rest of this paper is organized as follows. Section II describes the theory and design of the EME microstrip leaky line. Section III reports the corresponding scattering analyses, dispersion curves and modal current distributions to illustrate the properties of the proposed leaky-mode configuration. In Section IV, an experiment is performed to validate the reported numerical results and to present the attractive features of the EME microstrip. Conclusions are finally made in Section V.

## II. Design And Operation Of The EME Microstrip Leaky Line

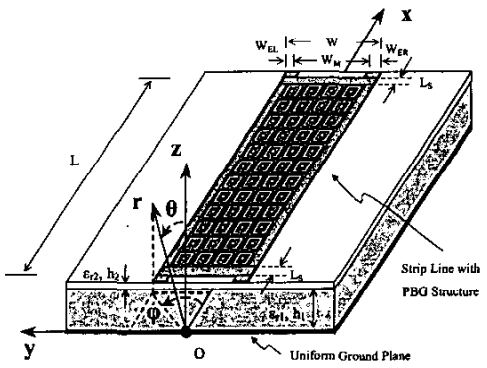


Fig. 1. Geometry structure of the EME microstrip leaky line. $\varepsilon_{r1} = 3.38$, $h_1 = 0.508$ mm, $\varepsilon_{r2} = 3.38$, $h_2 = 0.203$ mm, $L_S = 0.5$ mm, and $W = 8.536$ mm.

The EME microstrip [9]-[10] is like a conventional microstrip on a continuous, uniform ground plane except in that the signal line consists of composite metals made of electric-magnetic-electric conducting surfaces, as depicted in Fig. 1. The electrical surface is a plain, ordinary metal strip of a certain thickness. Coupled, connected metallic coils realize the magnetic surface. Each metallic coil is viewed as a unit cell. Thus, the coils form a periodic array in the central plane of the microstrip. The entire array resonates at a certain bandwidth, namely the stopband, and the connected metallic surface enters a high-impedance state [9]-[10]. In the design presented here, the unit cell is 2.134 mm wide (6% of free-space wavelength at 8.5 GHz), in both the x- and y-directions. The lower corner frequency of the anisotropic PBG structure, although



0-7803-7239-5/02/$10.00 © 2002 IEEE

varying with directions, is fluctuating around 8.5 GHz for our particular case study. The dispersion characteristics of the EME microstrip near and beyond the stopband are outside the scope of this paper.

The proposed guiding structure is symmetrical about its central plane, which is an electric wall for the microstrip odd-mode operation. Note that the magnetic surface is frequency-dependent, implying that the impedance of the magnetic surface is sufficiently high at a certain frequency band. The presence of the frequency-dependent magnetic surface at the central plane alters the modal current distributions along the transverse and longitudinal directions of the guide, thereby changing the dispersion characteristics. Proper widths ($W_{EL}$, $W_{ER}$ and $W_M$) of the electric and magnetic surfaces, respectively, can be chosen to obtain the required propagation constant, operating frequency and useful bandwidth of the leaky-mode antenna. This paper, however, focuses on a magnetic-surface (MS) microstrip with 100% PBG structure filling the metal strip, that is, $W_{EL} = W_{ER} = 0$.

The EME microstrip is constructed using conventional multilayer printed circuit technology. Referring to Fig. 1, the electric and magnetic surfaces are made on a two-sided, printed RO4003™ circuit board of thickness ($h_2$) 0.203 mm and relative permittivity ($\varepsilon_{r2}$) 3.38; the EME composite strip is then glued to a conductor-backing RO4003™ substrate of thickness ($h_1$) 0.508 mm under proper heat and pressure.

## III. Characteristics Of The EME Microstrip Leaky Line

### *A. Scattering Analyses*

One EME microstrip prototype with $W_M$ = 8.536 mm, corresponding to four cells in the transverse direction without electric surface, is analyzed. The EME microstrip is 32.01 mm long (L), corresponding to fifteen unit cells. A short, 0.5 mm long ($L_S$) metal strip is added at each end of the EME microstrip to facilitate the connection to the feeding structure. The small, uniform microstrip feed line is 1.6 mm wide and 0.5 mm long, corresponding to a 50 Ω microstrip on the combined substrates.

We first conduct the scattering analyses of the EME microstrip by differential excitations. Figure 2 shows the theoretical results obtained by a full wave integral equation solver. The radiation efficiency of the EME microstrip can be predicted by the relative power absorbed (RPA) calculation, which is defined as $1-|S_{11}|^2-|S_{21}|^2$. It should be noted that the conductor loss and the dielectric loss are not separated from the leakage power in the RPA calculation. The RPA results show that there are two peak regions of efficiency greater than 30%, which imply that large energy leaks away. The first peak RPA frequency is near 5.35 GHz (point d); the second is at 8.0 GHz, which is close to the lower corner of the stopband frequency of the PBG structure. Outside the frequency range between 5 GHz and 8.5 GHz, the reflection coefficient is nearly unity, the transmission coefficient is lower than –30 dB, and the RPA value is lower than 10%.

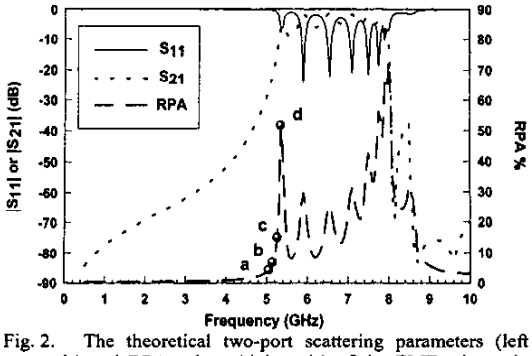


Fig. 2. The theoretical two-port scattering parameters (left axis) and RPA values (right axis) of the EME microstrip with differential excitations. L=32.01mm.

### *B. Dispersion Characteristics*

The excited electromagnetic waves propagated on the EME microstrip are the superposition of space harmonics due to the presence of periodic, magnetic surface. These space harmonics can be extracted by the matrix-pencil method [9]-[11]. The space harmonic is denoted by its complex propagation constant $\gamma_{m,n}^{\pm}$ ( $\alpha_{m,n}^{\pm} + j\beta_{m,n}^{\pm}$ ), which represents a traveling-wave component of the $n$th higher-order space component associated with the microstrip $EH_m$ mode: superscript + (-) signifies the forward- (backward-) traveling wave. Matrix-pencil analyses of the particular EME microstrip show that a forward traveling wave, denoted by its complex propagation constant $\gamma_{1,0}^{+}$, and a backward traveling wave, denoted by $\gamma_{1,0}^{-}$, are the only two major space harmonics for operating frequencies between 5.45 GHz and 8 GHz. Both $\gamma_{1,0}^{+}$ and $\gamma_{1,0}^{-}$ have the same values, but with opposite signs. Outside this frequency range, only the forward traveling wave $\gamma_{1,0}^{+}$ has significant contribution to the total field due to the high attenuation constant.

Figure 3 shows the normalized dispersion curves of the forward traveling wave component for the EME microstrip. The onset frequency of the leaky mode is at approximately 5.45 GHz, above which the normalized phase constant is greater than unity and the normalized attenuation constant is negligible for the particular case

study. The onset frequency of the EME microstrip is lower than that of the uniform microstrip with the same strip width (W) of 8.536 mm. In other words, the physical width is 47.5% less than that of a conventional microstrip, needing 16.256 mm for the same 5.45 GHz onset frequency.

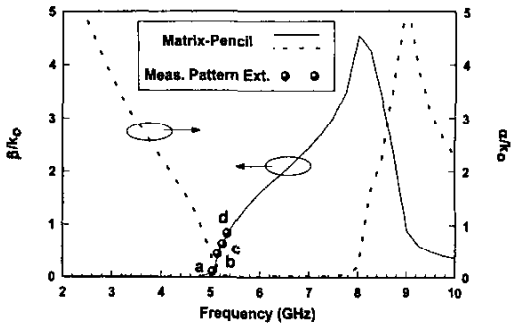


Fig. 3. The normalized phase constant $\beta/k_0$ (left axis) and normalized attenuation constant $\alpha/k_0$ (right axis) of the leaky mode for the EME microstrip.

Below the onset frequency, the first higher order mode becomes leaky, with its attenuation constant increasing as the frequency decreases. Consequently, we can observe that the EME microstrip depicts a strong radiation behavior between 5.05 GHz and 5.45 GHz, as shown in Fig. 2.

Above 5.45 GHz, the normalized phase constant curve enters the bound mode region, which is a slow wave with the normalized phase constant larger than unity and increasing with frequency toward 8.0 GHz. Thus the dips of $|S_{11}|$, as shown in Fig. 2, are caused by the bound modes resonating back and forth on the EME microstrip, and the period of adjacent dips is reduced with increasing frequency.

If the frequency is increased further beyond 8 GHz, the propagation constant becomes complex values with decreasing normalized phase constant and increasing normalized attenuation constant, until this curve enters a leaky region again, which is a fast wave with a complex propagation constant. However the leaky mode is not easily excited in this region because of high decay rates ($\alpha/k_0 > 1$). These findings correlate well with the scattering analyses as observed in Fig. 2.

### *C. Current Distributions*

It is of great interests to examine the modal current distributions of the leaky mode reported in Fig. 3. Figure 4 plots the transverse and longitudinal modal currents on the ground plane of the EME microstrip at 5.25 GHz (point c in Fig. 2 and Fig. 3). Currents are normalized to have a maximum value of unity. The real and imaginary parts of the longitudinal current (Jx) are odd-symmetric and have null values at the central x-z plane. The real and imaginary parts of the transverse current (Jy) are even-symmetric and have maximum values at the central plane. Also, the imaginary part dominates the transverse current. Thus the modal current distributions of the EME microstrip agree with those of the first higher order microstrip leaky $EH_1$ mode.

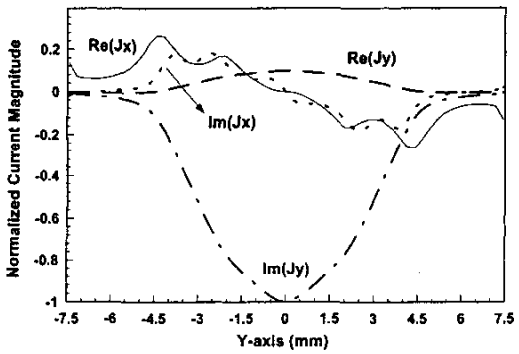


Fig. 4. Normalized current distributions of the first higher order leaky mode for the EME microstrip at 5.25 GHz. The normalized propagation constant is around $\gamma = 0.06 + j0.67$.

## IV. Experimental Results And Validity Checks

We are not surprised to see that the far field radiation patterns and frequency-scanning property of the EME microstrip are almost identical to that of the uniform microstrip in the leaky region. Based on the theoretical analyses outlined in the previous section, an EME leaky-mode antenna is fabricated and tested. The experimental antenna is fed asymmetrically with a 50 Ω microstrip. The antenna has the same dimensions as reported in Fig. 1 with the length (L) of 256.08 mm, corresponding to 4.5 $\lambda_0$ (free-space wavelength at 5.25 GHz). This length is larger than the required 3.9 $\lambda_0$ if more than 90% of the electromagnetic energy will leak [2].

Next, we conduct the H-plane (the x-z plane) radiation pattern measurement in an anechoic chamber. The particular design leaks in a fan beam fashion below the onset frequency at 5.45 GHz. The phase constant can be extracted from the measured radiation pattern, as the leaky mode radiates with a main beam angle at $\theta_m \approx \sin^{-1}(\beta/k_0)$, measured from the broadside direction (z-axis) [5]. The measured values, in circle symbols, are superimposed to the normalized phase

constant curve of Fig. 3, showing excellent agreement has been achieved for the four measured frequencies marked as points a, b, c and d.

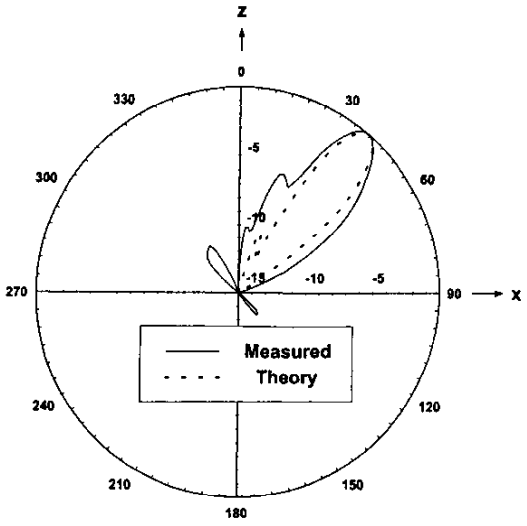


Fig. 5. The far field H-plane radiation pattern of the asymmetrically-fed EME microstrip leaky-mode antenna at 5.25 GHz. L=256.08 mm.

Furthermore, the radiation pattern of the leaky line can be directly derived from the extracted complex propagation constant [5]. Figure 5 indicates that the theoretical and measured copolarization far-field patterns along the H-plane are in good agreement at 5.25 GHz (point c). The main beam angle agrees to less than 1.5° difference and the measured beamwidth is a slightly broader than the theoretical prediction.

## V. Conclusion

This paper presents the dispersion characteristics of the EME microstrip that incorporates a uniform grounded substrate and uses PBG structures alongside the signal line in the axial direction. The leakage, produced by the excitation of the first higher order (odd) microstrip mode, and the dispersion curves, obtained by matrix-pencil analyses, are validated by measured radiation patterns. Theory and experiments show that the physical dimension of the EME leaky line is reduced significantly by 47.5%, compared to the conventional uniform microstrip on the same substrate. This result implies that the aperture efficiency of the leaky-mode antenna array can be improved by the proposed EME structure. The implementation of the EME composite strip in the integrated circuit and antenna structures may open up many possibilities of designing useful and compact devices.

## Acknowledgement

This work is supported by National Science Council of Taiwan under contract NSC 90-2213-E-009-063 and in connection to project Advanced Technologies for Telecommunications (A) under contract 89-E-FA06-2-4.

## References

[1] F. Schwering and S. T. Peng, "Design of dielectric grating antennas for millimeter-wave applications," *IEEE Trans. Microwave Theory Tech.*, vol. MTT-31, pp. 199-209, Feb. 1983.

[2] A. A. Oliner, "Leakage from higher modes on microstrip line with application to antennas," *Radio Sci.*, vol. 22, no. 6, pp. 907-912, Nov. 1987.

[3] H. Y. D. Yang, N. G. Alexopoulos, and E. Yablonovitch, "Photonic band-gap materials for high-gain printed circuit antennas, " *IEEE Trans. Antenna Propagation*, vol. 45, pp. 185-187, Jan. 1997.

[4] H. Y. D. Yang and D. R. Jackson, "Theory of line-source radiation from a metal-strip grating dielectric-slab structure," *IEEE Trans. Antenna Propagation*, vol. 48, pp. 556-564, Apr. 2000.

[5] G. J. Chou and C. K. C. Tzuang, "Oscillator-type active-integrated antenna: the leaky-mode approach," *IEEE Trans. Microwave Theory Tech.*, vol. MTT-44, pp. 2265-2272, Dec. 1996.

[6] C. N. Hu and C. K. C. Tzuang, "Analysis and design of large leaky-mode array employing the coupled-mode approach," *IEEE Trans. Microwave Theory Tech.*, vol. MTT-49, pp. 629-636, Apr. 2001.

[7] D. Sievenpiper, L. Zhang, R. F. J. Broas, N. G. Alexópolous, and E. Yablonovitch, "High-impedance electromagnetic surfaces with a forbidden frequency band," *IEEE Trans. Microwave Theory and Tech.*, vol. 47, pp. 2059-2074, Nov. 1999.

[8] F. R. Yang, K. P. Ma, Y. Qian, and T. Itoh, "A uniplanar compact photonic-bandgap (UC-PBG) structure and its applications for microwave circuits," *IEEE Trans. Microwave Theory and Tech.*, vol. 47, pp. 1509-1514, Aug. 1999.

[9] C. K. Wu and C. K. Tzuang, "Slow-wave propagation of Microstrip Consisting of Electric-Magnetic-Electric (EME) Composite Metal Strips," *2001 IEEE MTT-S Int. Microwave Symp. Dig.*, vol. 2, pp. 727-730, May 2001.

[10] C. K. Wu, H. S. Wu and C. K. Tzuang, "Electric-Magnetic-Electric (EME) slow-wave microstrip line and bandpass filter of compressed size," *to appear in the August 2002 issue of the IEEE Trans. Microwave Theory and Tech.*

[11] Y. Hua and T. K. Sarkar, "Generalized pencil-of-function method for extracting poles of an EM system from its transient response," *IEEE Trans. Antenna Propagat.*, vol. 37, pp. 229-234, Feb. 1989.